Available online at www.sciencedirect.com

ScienceDirect

Procedia Structural Integrity 2 (2016) 681–689

Structural Integrity Procedia

www.elsevier.com/locate/procedia

21st European Conference on Fracture, ECF21, 20-24 June 2016, Catania, Italy

Fatigue investigation at high load ratio R of a quenched and tempered chromium molybdenum steel

L. Bertini[a], L. Le Bone[a], C. Santus[a], F. Chiesi[b], L. Tognarelli[b]

[a] *Università di Pisa – Dipartimento di Ingegneria Civile e Industriale, Largo L. Lazzarino2, Pisa 56126, Italy*
[b] *GE Oil&Gas – Nuovo Pignone S.p.A, Via F. Matteucci, Firenze 50127, Italy*

Abstract

The fatigue behavior at high number of cycles in elastic-plastic field of quenched and tempered carbon chromium steel was experimentally investigated for high performance reciprocating compressors application. Fatigue tests on un-notched specimens were performed both under load and strain controls, by imposing different levels of stress/strain and for each of them different values of stress ratios R, especially high values. Stress and strain trends have been monitored, during the fatigue life, and either ratcheting or relaxation, respectively, was evident.
The stress control tests have resulted into fatigue fractures only for low values of R with significant ratcheting and an increasing rate during the final part of the test, thus the fracture could be considered as a synergy between fatigue damage and plastic failure. On the contrary, the ratcheting stabilized for high values of R and the tests were finalized without any fracture. Within an intermediate region, for medium/high values of R, a minor ratcheting and the fracture transition have been found. Similarly, for the tests under strain control, low values of R showed fatigue fractures despite a considerable relaxation, conversely for high values of R, the relaxation was limited without any fracture. After reporting the tests on the Haigh plane, the Smith-Watson-Topper equation (SWT) provided the best prediction of the fatigue strength, at least until the intersection with the ultimate stress line, both under stress and strain control loadings. The cyclic behavior of the material was then investigated through several static and cyclic tests on plain specimens. A kinematic hardening Chaboche model, with three parameter couples, was proposed and the values of these parameters derived and discussed. Finally, other tests have been conducted on notched specimens with C geometry and blunt radius, again at high R values. FE analysis allowed the prediction of the stress evolution during the loading cycling, implementing the Chaboche model, and observing a combined effect of ratcheting and relaxation at the notch tip. The stabilized stresses were finally reported on the Haigh diagram and the results were found in agreement with the plain specimen fatigue line.

Keywords: "Fatigue, High Ratio R, Ratcheting, Relaxation, Chaboche, notched specimens"

Copyright © 2016 The Authors. Published by Elsevier B.V. This is an open access article under the CC BY-NC-ND license (http://creativecommons.org/licenses/by-nc-nd/4.0/).
Peer review under responsibility of the Scientific Committee of ECF21.
10.1016/j.prostr.2016.06.088

1. Introduction

The effect of mean stress σ_m on fatigue has been extensively studied for tensile mean stress values less than about 60% of the ultimate strength and R ratio less than 0.5 approximately (Forrest PG (1962), Stephens et al. (2000)). A comprehensive literature investigation resulted in a very few papers dealing with high tensile mean stresses and high R ratio for un-notched or notched specimens (Howell and Miller (1955), Bell and Benham (1962), Morrissey et al. (1999) and Maxwell and Nicholas (1999)). However, many mechanical components experience a high tensile mean stress superimposed to a small alternating stress (high R ratio) such as pre-tightened axially loaded bolts, gas turbine blades and aircraft wings. Design engineers are expected to predict the fatigue life of components under a high mean tensile stress and a high R ratio despite the absence of significant research and understanding of these conditions. The objective of this research is to study the high mean stress effect of 42CrMo4 steel, by imposing different levels of stress/strain and for each of them different values of stress ratio R, especially high values (R>0.5) under load and strain control (Karadag and Stephens (2003) and Pals and Stephens (2004)). The material has been obtained from the rod of a reciprocating compressor characterized by a diameter approximately 130 mm and a length of 1500 mm. Stress and strain trends have been monitored, during the test for investigating either ratcheting or relaxation. Other tests have been conducted on notched specimens with stress concentration factor k_t=1.65. The base material behavior was initially investigated through static and cyclic tests, and then a Chaboche model with three parameter couples was proposed to analyze the evolution of the stress at the tip of the notch after the first cycle and subsequent stabilizing initial cycles.

2. Material characterization

2.1. Static characterization: tensile test

Fig. 1 show engineering stress-strain curves derived from a tensile test. This curve allows evaluating the tensile properties of the material and the tensile test obtained parameters are listed in Tab. 1.

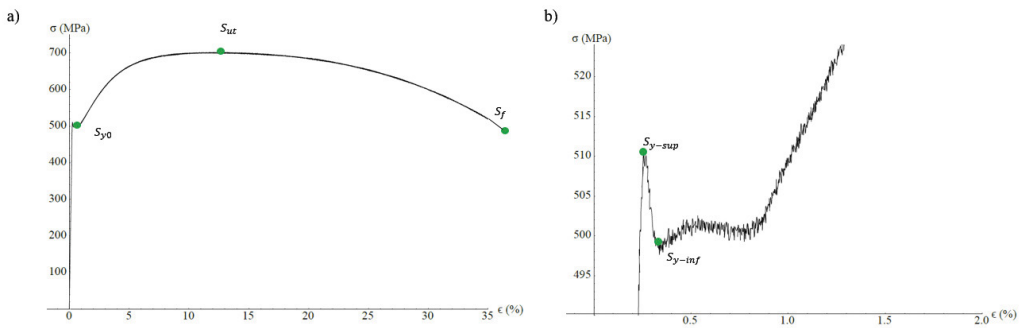

Fig. 1. (a) Engineering stress-strain curve; (b) detail of yelding “point”

Table 1. Tensile test parameters.

E (GPa)	S_{y0} (MPa)	$S_{y-\sup}$ (MPa)	$S_{y-\inf}$ (MPa)	S_{ut} (MPa)	ε_{ut}	S_f (MPa)	ΔL (%)	RA (%)
209	500	511	499	700	0.123	467	32	64

The stress-strain curve has been obtained from quasi-static tests conducted on standard specimens using a servo-hydraulic machine with axial load capacity of 250 kN. The tests have been conducted in laboratory at room temperature with constant displacement rate. The instantaneous elongation of the sample has been measured by using an extensometer attached on the specimen.

The stress σ_t (true) rather was evaluated and considered, rather than the engineering stress σ, for a more direct measure of the material's response in the plastic flow range. Fig. 2 shows the true stress-strain curve, superimposed to the engineering curve, and the related parameters are reported in tab. 2.

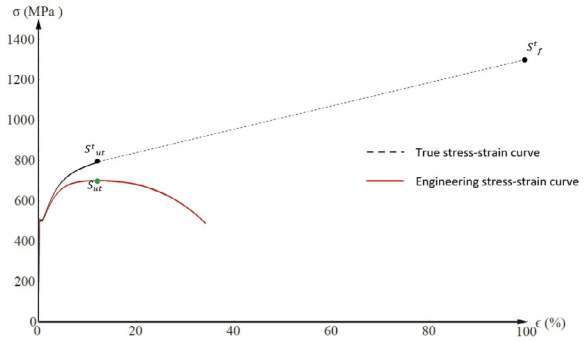

Fig. 2. Engineering and True stress-strain curves.

Table 2. Parameters tensile test

S^t_{ut} (MPa)	S^t_f (MPa)	ε^t_{ut} (%)	ε^t_f (%)
787	1300	12	100

2.2. Cyclic characterization

In order to cyclically characterize the material, several deformation (strain) control tests have been performed: 4 load steps have been imposed to gradually bring the material in the plastic range. The values of stresses and strains in the various load steps are listed in Tab. 3

Table 3. Stress and strain values at various steps.

	Step 1	Step 2	Step 3	Step 4
$\Delta\varepsilon$ (%)	± 0.2	± 0.5	± 1	± 2
$\Delta\sigma$ (MPa)	± 380	± 500	± 510	± 580

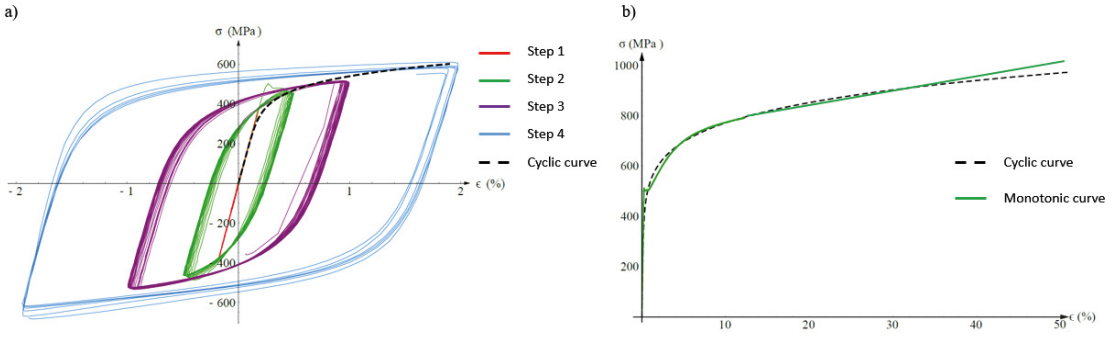

Fig. 3. (a) Hysteresis loops measured during the tests and cyclic curve (dashed), (b) comparison between the cyclic curve (dashed) and monotonic tensile curve (green).

Fig. 3(a) shows the hysteretic loops obtained experimentally at the different cyclic strains then used to obtain the cyclic stress-strain curve of the material. A useful representation of the cyclic stress-strain curve was obtained with the Ramberg-Osgood equation:

$$\varepsilon = \frac{\sigma}{E} + \left(\frac{\sigma}{k}\right)^{\frac{1}{n}}$$

and the values of *K* and *n* are, respectively: 1070 MPa and 0.14.
As evident in Fig. 3 (b) the monotonic and the cyclic curves showed very similar trends, thus without any significant hardening of softening.

2.3. Identification of the Chaboche's hardening model parameters

The model considered in the present work is a generalization of the linear kinematic rule introduced by Prager (Prager (1956)), where the yield surface is given by the following function:

$$f = f(\sigma - X) - \sigma_Y = 0 \tag{1}$$

Chaboche (1986) and Chaboche et al. (1979) proposed their decomposed hardening rule in the following form:

$$X = \sum_{i=1}^{m} X_i \qquad dX_i = \frac{2}{3} C_i d\varepsilon_p - \gamma_i X_i dp$$

Where C_i and γ_i are the couples of material parameter (Chaboche's parameters), to be identified. The number of parameter couples considered was m=3. Two kinds of experiments were required to perform the identification: one strain controlled hysteresis curve and one stress controlled. In order to find the Chaboche's parameters three hysteretic loops have been take into account, Fig 3(a): $\varepsilon_{max} = \pm 0.5$ %, $\varepsilon_{max} = \pm 1$ % and $\varepsilon_{max} = \pm 2$ % , plus a stress controlled test at R=-0.66 with $\sigma_{max} = 600$ MPa as shown in Fig. 4.

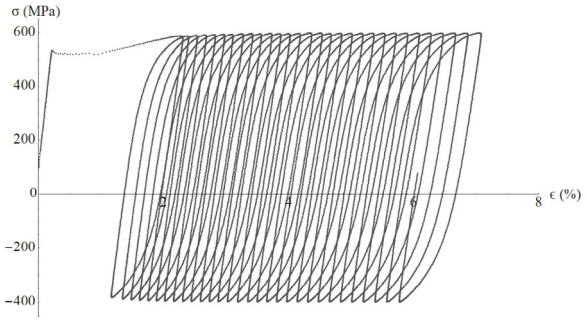

Fig. 4. Stress controlled test with R=-0.66 and σ_{max} = 600 MPa for the determination of the Chaboche's parameters.

In this study the yield stress has been used as an extra parameter, thus differentiating the yield stress (engineering, 0.2% offset) obtained from the tensile test. After an optimization calculation, the Chaboche's parameters obtained from these tests are listed in Tab 4.

Table 4. Chaboche's parameters.

	C_1 (MPa)	γ_1	C_2 (MPa)	γ_2	C_3 (MPa)	γ_3	S'$_{y0}$ (MPa)
Parameter	21746	16704	103651	518	7688	6.1	258

Fig. 5 (a) shows the mean strain as a function of the number of cycles both from the experimental data and the analytical model, while Figs. 5 (b) and (c) show the experimental stabilized hysteresis loops at ε_{max} =±0.5% and ±1.0% (only the plastic strain component is reported in the horizontal axis of figures (b) and (c)). It is evident that the experimental trends are accurately reproduced by the material model after finding an optimization point between the ratcheting (not-symmetric) and the alternating (symmetric) cyclic tests.

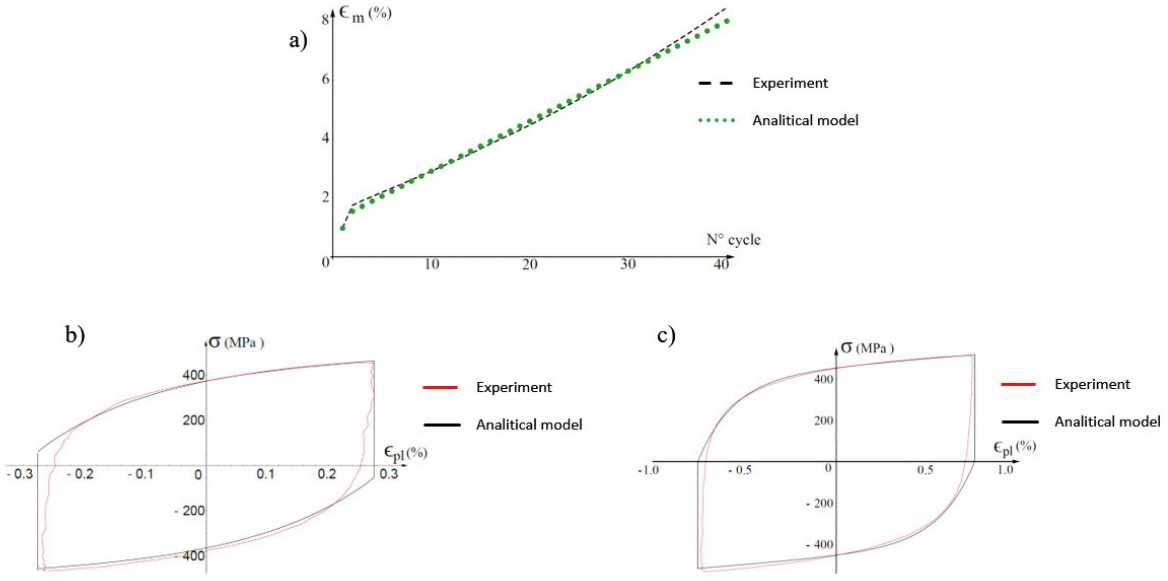

Fig. 5. (a) Comparison between experimental data and Chaboche's analytical model: ratcheting mean strain for not-symmetric loading (a), stabilized hysteresis loops at ε_{max}=±0.5% (b) and ε_{max}=±1% (c).

3. Fatigue tests

The material fatigue strength has been investigated with 42 tests on un-notched specimen, among them 31 under stress control to study the phenomenon of the accumulation of plastic strain (ratcheting) while the remaining 11 in strain control to study the relaxation (Guozheng (2009)).

For both the tests under stress and strain control, 3 levels of maximum stress have been considered: 650 MPa; 600 MPa and 550 MPa, between the yielding stress S_{y0} and the ultimate stress S_{ut}, and 7 levels of load ratio R (R=0; 0.1, 0.2; 0.3; 0.4; 0.5; 0.6; 0.7 and 0.8) plus the reference case at R=-1. The experiments were conducted in a closed-loop servo-hydraulic test machine (Schenck 250 kN) with an axial load capacity of 250 kN. The load was monitored through a calibrate load cell, and strain was with an extensometer controlling either the load or the extensometer strain.

Finally, the notched specimen test series have been conducted to obtain the fatigue limit at five load ratios: R=-1; R=0; R=0.3; R=0.5 and R=0.7, obviously under load control only.

3.1. Load control test results

The tests performed under load control on plain specimens, as shown in Fig. 6, resulted as fatigue fractures for low values of R (R<0.3), given that at the high load ratios the alternating component was necessarily reduced due to the limitation imposed by the ultimate stress line. Comparing the results with various models, as shown in figure, only the Smith-Watson-Topper (SWT) equations provided the accurate prediction on the fatigue results of the component, at least until the intersection with Gerber's parabola.

For low values of R, the fatigue test resulted in a significant ratcheting with increasing rate during the final part of the test, leading to a fracture after an evident necking despite σ_{max} was lower than S_{ut}. The fracture in this case can be considered as a combination of fatigue damage and plastic yielding. Some of the mean strain trends as function of the number of cycles, for R=0.1; 0.3 and 0.7, are reported in Fig. 7. For high values of R (R>0.5), as showed in Fig. 7 (c)-(f), referred to the case R=0.7, the ratcheting stabilized and the tests were completed without failure. In an intermediate area, for medium/high values of R between 0.3 and 0.5, a minimum ratcheting and fracture transition was found.

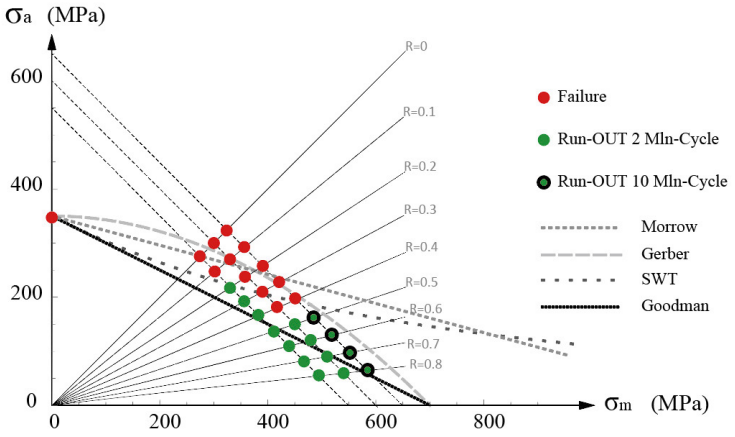

Fig. 6. Results of the tests under stress control on the Haigh diagram and comparison with various predicting fatigue models.

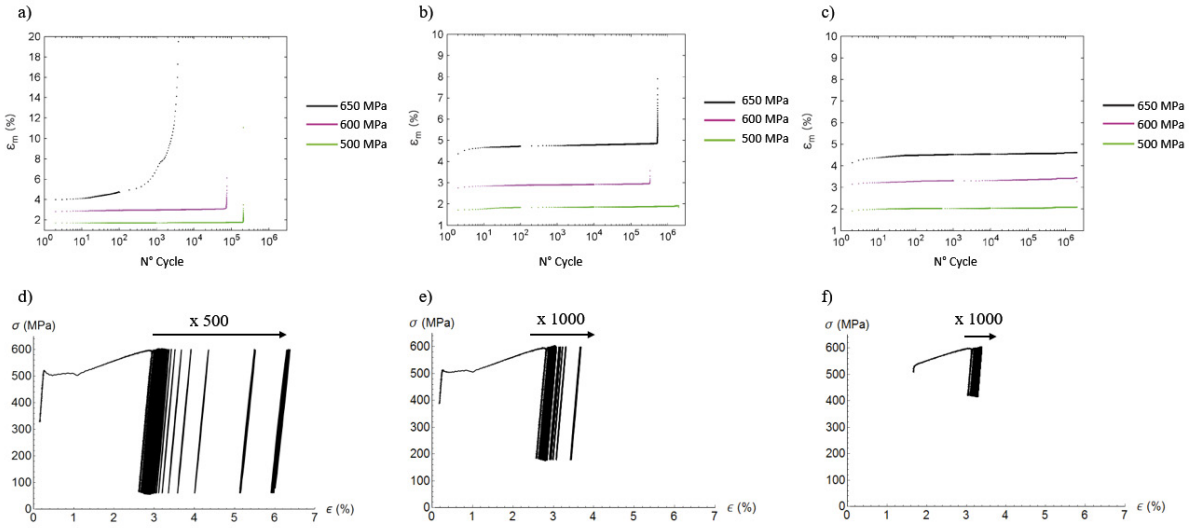

Fig. 7. (a) - (b) - (c) Mean strain as function of the number of cycle for R =0.1; 0.3 and 0.7 respectively with σ_{max}=600 MPa. (d) - (e) - (f) Stress-strain for the same tests at different number of cycles.

3.2. Strain control test results

Since the strain was imposed for this kind of test to obtain a specific initial combination of maximum and minimum stresses, the mean stress reduced after the first cycle due to the relaxation. Fig. 8 shows the trends of the mean stress as function of the number of cycles for the tests with maximum stress of 600 MPa and load ratios

ranging from R=0 and R=0.8. Similarly to what happened for the load control tests, fatigue failures were found only for low values of R in spite of a significant relaxation, Fig. 9. No failures were obtained for high values of R along with a very limited relaxation. Therefore, a fracture transition zone was again found at approximately R=0.3. The SWT equation, again, very accurately defined the fatigue limit. Indeed, those tests below this curve ended without a failure, even being beyond the Goodman's line, while the tests initially above experienced fatigue fracture though the relaxation moved these points approximately on the SWT line itself.

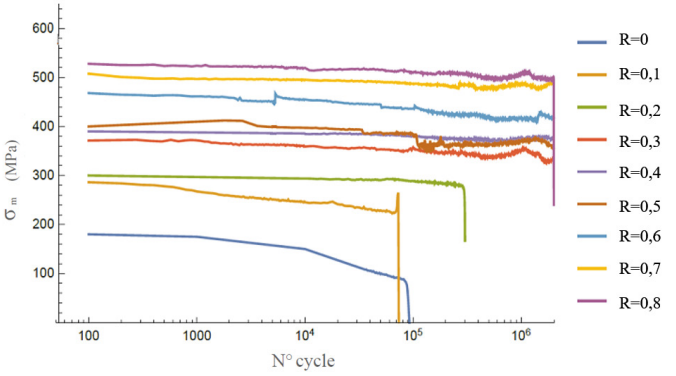

Fig. 8. Mean stress relaxation with σ_{max}=600 MPa and different load ratios.

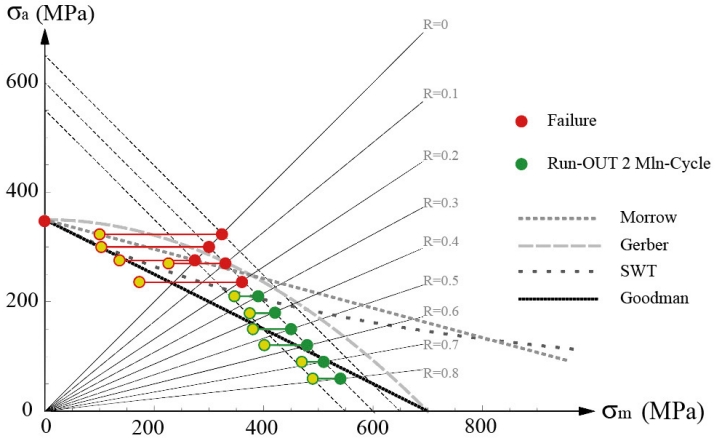

Fig. 9. Results of the strain control tests, showing relaxation, and comparison with various fatigue models.

3.3. Notched specimen test results and local stress prediction

The tests conducted on notched specimens, shown in Fig. 10, with stress concentration factor k_t=1.65, have been carried out on a resonance fatigue machine (150 Hz), testing different series to obtain the fatigue limit at R = -1; 0; 0.3; 0.5 and 0.7.

These fatigue limit values were then used as input in a FE model (ANSYS software), using the previously found Chaboche's parameters, in order to evaluate the local stresses at the notch root and the evolution during the number of cycles. The notch root stresses for the fatigue limits are shown in Fig. 10. The hollow circles with larger size represent the mean and the alternate nominal stresses times the k_t factor, while the smaller size hollow circles represents the stresses (mean and alternate), as calculated by the FE model at the first load cycle. Finally, the solid

circles represent the stresses provided by the numerical calculation after the relaxation predicted by the linear kinematic model. This stabilization settled the mean and alternate stress points very close to the SWT curve, intersected with the Gerber's parabola, thus confirming the accuracy of the predictive approach.

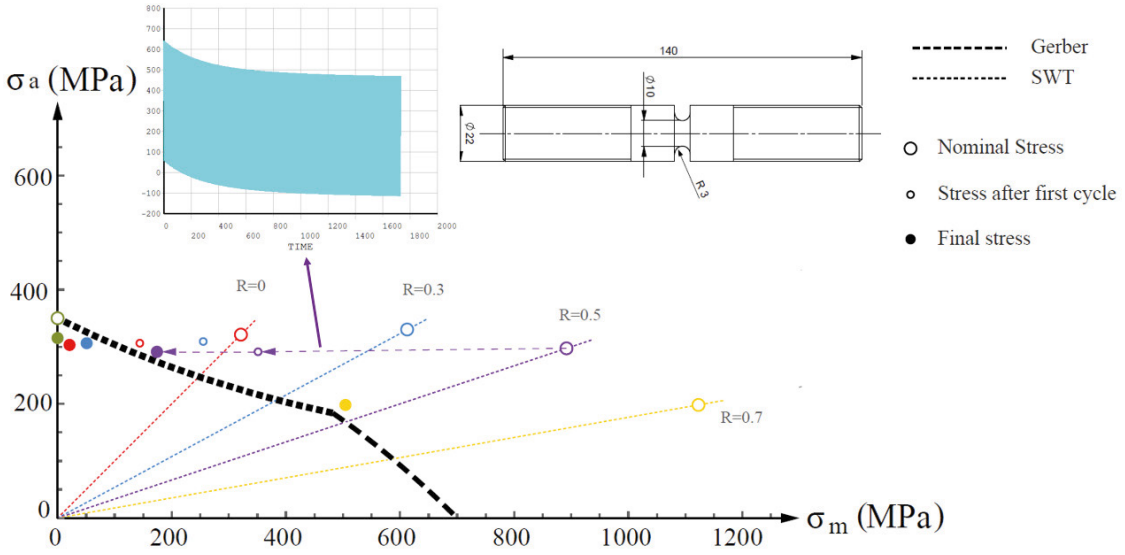

Fig. 10. FE simulated stress points of the notched specimens on the Haigh diagram and agreement with the SWT prediction.

4. Conclusions

This work reported a complete characterization of the material 42CrMo4 from the fatigue behavior, ratcheting and relaxation, especially for high *R* values.

This steel, with the provided heat treatment condition, showed the yield strength at 500 MPa, defined as 0.2% offset, but an unstable behavior for the amplitude values of the stress lower than the elastic limit given by tensile test. Therefore, the Chaboche model, also introducing the yield stress as a free parameter, resulted in an elastic limit values significantly lower (258 MPa).

For un-notched specimen, moving in the Haigh diagram, and not being able to exceed the ultimate stress S_{ut}, a high ratcheting for low R values, slightly above zero, was observed and again for higher R values (0.7 and 0.8). In the first case the alternating component has a predominant role, while in the second case, the mean stress is more significant. In addition, for low R values, the ratcheting causes the failure of the specimen with evident necking and no fatigue component in the fracture surface. On the contrary, for higher R values, approximately 0.3, the necking disappeared and it was possible to recognize a typical fatigue surface. The results showed the validity of the Smith-Watson-Topper model, at least until the intersection with the Gerber's parabola. Finally, simulations carried out with the FE model on the notched specimen, showed stress stabilization very close to the SWT line intersecting the Gerber's parabola thus demonstrating the predictive validity of the developed numerical model.

References

Forrest PG, 1962 Fatigue of metals. London: Pergamon Press.
Stephens RI, Fatemi A, Stephens RR, Fuchs HO,2000. Metal fatigue in engineering, 2nd ed. NY: Wiley Interscience.

Howell FM, Miller JL.,1955. Axial-stress fatigue strengths of several aluminum alloys. Proceedings of American Society for Testing Materials, vol. 55. West Conshohocken, PA: American Society for Testing Materials. p. 955–68.

Bell WJ, Benham PP.,1962. The effect of mean stress on fatigue strength of plain and notched stainless steel sheets in the range of 10 to 10^6 cycles. Symposium on Fatigue Tests of Aircraft Structures: Low-Cycle, Full-Scale, and Helicopters, STP 338. West Conshohocken, PA: American Society for Testing and Materials. p. 25–46.

Morrissey RJ, McDowell DL, Nicholas T.,1999. Frequency and stress ratio effects in high cycle fatigue of Ti–6Al–4V. International Journal of Fatigue 21, 679–85.

Maxwell DC, Nicholas TA,1999. Rapid method for generating a Haigh diagram for high cycle fatigue. In: Panontin TL, Sheppard SD, editors. Fatigue and fracture mechanics. ASTM STP 1332, vol. 29. West Conshohocken, PA: American Society for Testing and Materials; p. 626–41.

M. karadag, R. I. Stephens, 2003. The influence of high R ratio on unnotched fatigue behavior of 1045 steel with three different treatments. International Journal of fatigue 25 191-200.

T.G. Pals, R.I. Stephens, 2004. The influence of high ratio on mild and sharp notched and unnotched fatigue behavior of 1045 steel with three different treatments. International journal of fatigue 26 651-661.

Prager, W., 1956. A new method of analysing stresses and strains in work hardening plastic solids. J. of Applied Mechanics 23, 493-496.

Chaboche J.L., 1986. Time independent constitutive theories for cyclic plasticity. International journal of Plasticity. 2, 149-188.

Chaboche, J.L., Dang-Van, K., Cordier, G., 1979. Modelization of the strain memory effect on the cyclic hardening of 316 stainless steel. Proc. of the 5th International Conference on SMiRT, Div. L, Berlin, Germany.

Guozheng Kang, Yujie Liu, Jun Ding, Qing Gao, 2009. Uniaxial ratcheting and fatigue failure of tempered 42CrMo steel: Damage evolution and damage-coupled visco-plastic constitutive model. International journal of Plasticity. 25, 838–860.